



A feasibility study for near-infrared spectroscopy with GeMS

Aurea Garcia-Rissmann^a, Eleazar Rodrigo Carrasco^a, Ruben Diaz^a, Joan Font^a, Vincent Garrel^a,
Manuel Gomez-Jimenez^a

^aGemini Observatory, NSF's NOIRLab, c/o AURA, Casilla 603 La Serena, Chile

ABSTRACT

As part of the AO-related upgrades envisioned for the Gemini Observatory a feasibility study has been started aiming to integrate GeMS with Flamingos-2 operations. This latter, hereafter referred to as F2, is a wide-field near-infrared imager, long-slit and multi-object spectrograph with a demand contribution among the Gemini South instruments currently ranging around 15-20%. The integration with GeMS can open the possibility for an AO-corrected beam to feed spectroscopic modes, thus significantly increasing the sensitivity and spatial resolution of F2 observations covering J, H and K bands. First steps towards this goal included a characterization of the current PSF centroid stability delivered by GeMS using the Gemini South Adaptive Optics Imager (GSAOI), followed by actual tests with the GeMS+F2 setup. A brief presentation of main aspects and challenges being addressed in this feasibility study is given, such as related to calibration issues, a revisit of the non-common path aberrations calibration strategy, background contribution and field distortion characterization. Results from preliminary operational settings and on-sky tests are presented.

Keywords: adaptive optics, multi-conjugate adaptive optics, near-infrared spectroscopy

1. INTRODUCTION

GeMS, the laser-assisted multi-conjugate adaptive optics (MCAO) system at the Gemini South telescope (Cerro Pachón, Chile) has been in operation for ~11 years (see [1][2] for details). The system has undergone a few major modifications over the years with the objective to improve its performance stability and to increase the sky coverage. Such efforts consisted mainly in the implementation of a 22W Toptica laser to substitute the original 50W LMCT diode-pumped solid-state unit, and the replacement of the original avalanche photodiode-based NGS WFS by an EMCCD-based one (named NGS2) in order to extend the sky coverage and tip-tilt sensitivity. It is worth noting that with the NGS2 commissioning the Peripheral Wavefront Sensor 1 (PWFS1) at the Acquisition and Guiding (A&G) telescope module was adopted as the slow focus sensor. The GeMS AO bench (Canopus) is mounted on a side port of the Instrument Support Structure (ISS); it receives the original F/16 telescope beam and outputs an AO-corrected F/32 beam¹, which translates into an unvignetted field-of-view (FoV) of ~2 arcmin diameter on the telescope focal plane. The laser constellation consists of 5 stars distributed in a X-shaped geometry, and observations can count on up to 3 natural guide stars for tip-tilt correction. The maximum loop rate is of 800 Hz for both LGS and NGS sensors (with the latter being set to a fraction of the former). Under good seeing and photon return conditions it has routinely been possible to achieve with this instrument an H-band FWHM resolution of 80 mas or better.

This MCAO system is currently used only with the Gemini South Adaptive Optics Imager (GSAOI, [3][4]), but it has been a long-term plan to use it to also feed spectroscopic modes, such as those provided by Flamingos-2 (F2), a near-infrared imager and spectrograph. This instrument counts on an extra capability to receive a F/32 beam and on 2 different Lyot stops to mitigate the thermal background contamination when observing towards redder wavelengths. F2 is currently used in seeing-limited F/16 mode for queue operations, with a semester proposal demand comprising around 15-20% of the total for instruments at Gemini South. Out of this fraction, the majority of the allocated time is used for

¹ The delivered F-number is actually closer to F/33, in contrast to the original intent for the design to provide F/32.

spectroscopy. More recently the multi-object spectroscopy (MOS) mode was commissioned for seeing-limited F2, covering a field of 6 arcmin x 2 arcmin. When working with the AO correction, the main goal is to obtain both F2 long-slit and MOS observations over J, H and K bands, with the unvignetted MOS area covering about half of the GeMS FoV (~ 1.6 arcmin²). Sharper point-spread functions will enable observations using narrower slits (such as ~ 0.18 arcsec), increasing the spectral resolution and the instrument efficiency for a given signal-to-noise ratio. Some expected performance items are:

- Centroid stability in 5 minutes: $r < 15$ arcsec ~ 0.05 arcsec; 40 arcsec $< r < 55$ arcsec ~ 0.15 arcsec
- FWHM stability: $r < 20$ arcsec $\sim 5\%$ and $r < 40$ arcsec $\sim 10\%$
- 50% EED ~ 0.15 arcsec, 80% EED ~ 0.35 arcsec (K_s , for IQ70 conditions)
- Imaging sensitivity in J, H, K_s : ~ 24.4 , 23.6 , 23.6 mag, respectively
- Long-slit 2-pix limiting magnitude: JH, HK: ~ 21.5 , ~ 21.3 mag
- Long-slit 2-pix spectral resolution for J, H, K_s , K-long: R ~ 3400 , R ~ 2300 (0.18 arcsec and 0.27 arcsec slit widths, respectively)
- F2+GeMS MOS # targets: ~ 80 objects (offset to sky), ~ 40 objects (ABBA short nodding)

In this paper we discuss the results from preliminary tests conducted at Gemini South, as well as the next steps needed for implementing the AO mode of operation for F2.

2. OPERATIONAL ASPECTS

Observing in the GeMS+F2 configuration requires the definition of a new set of operational procedures. Standard seeing-limited F2 observations have the telescope light reaching the science fold (SF) mirror located in the ISS, which redirects it to the instrument. Under the GeMS+F2 setup the AO fold mirror is introduced in a prior stage in the ISS, first redirecting the light to Canopus; the science light subsequently passes through several (static and deformable) mirrors and a dichroic, exits the bench and is then redirected to F2 by the SF mirror. Aligning the pupil of the AO instrument with the pupil of F2 can be done through the SF mirror; notice, however, that the alignment procedure also induces changes on the field pointing, impacting coordinate system calibrations. The definition of the instrument origin must be made once the alignment is done and is required for having the target to fall in proximity to a specified position on the instrument detector. Calibration parameters of the instrument are used by the telescope control system (TCS) which works in tandem with the observatory operational tools; the engineering nights described in this document have been used to make an assessment of the necessary software modifications, both on the user and on the observatory operational side.

Seeing-limited F2 observations use the GCAL calibration unit located at the ISS for acquiring internal flat and arc lamp calibrations. The GeMS+F2 configuration precludes the use of this unit because it cannot send light through Canopus, whose entrance shutter is located at a prior stage in the ISS. As a consequence, the adopted strategy for wavelength calibration during engineering nights consisted in observing OH sky lines and calibrating them through the Rousselot catalog [5], which turned out to be satisfactory. Regarding flat-field frames, for the data presented here we used dome flats taken with the lamps normally used for GSAOI calibrations. The flexure stability of such flat-field calibrations has yet to be addressed, but a possible alternative would consist in implementing a calibration source inside Canopus at the NGS calibration source level. Telluric stars for calibrations can be observed without laser propagation, counting solely on tip-tilt corrections coming from NGS2.

3. ON-SKY TESTS

3.1 First assessment: AO-correction centroid stability

GeMS and GSAOI were used in half a night of engineering in January 2023 for checking the centroid stability on the science images, both spatially and temporally. The weather conditions were not optimal, with degrading seeing and low photon return leading to lower loop rates (< 300 Hz), so we can assume the results shown here to indicate a lower limit in performance. The observed target, the cluster NGC 1851, was tracked in airmasses close to 1.0 for ~ 1 h period. Images

of 60 seconds in the H-band were acquired in a sequence, only interrupted by a large sky offset of over 5 arcmin before taking the last 5 images. Analysis point to (H-band) Strehl ratios varying between 8-13% during these observations.

Figure 1 shows the standard deviations on the centroid measurements in X and Y directions (corresponding to E-W and N-S directions, respectively). Maximum peak-to-valley centroid values of 0.046 and 0.048 arcsec were obtained for these two axes, respectively, and confirm a slightly better performance in the X direction. Figure 2 shows the time evolution, in this sequence, of the measured centroids for the selected stars in the 4 GSAOI quadrants. The degrading performance as the observations progressed are reflected in degraded PSFs, and in turn in the centroid measurement errors. Ongoing work on the realignment of the LGS WFS optics as well as the careful re-calibration of the anisoplanatic modes loop aim to address this issue. In addition, closeness to transit may also have had an impact in the results: having the target to pass very close to Zenith can pose an extra challenge for the Cassegrain rotator tracking, and the loop stability can be affected.

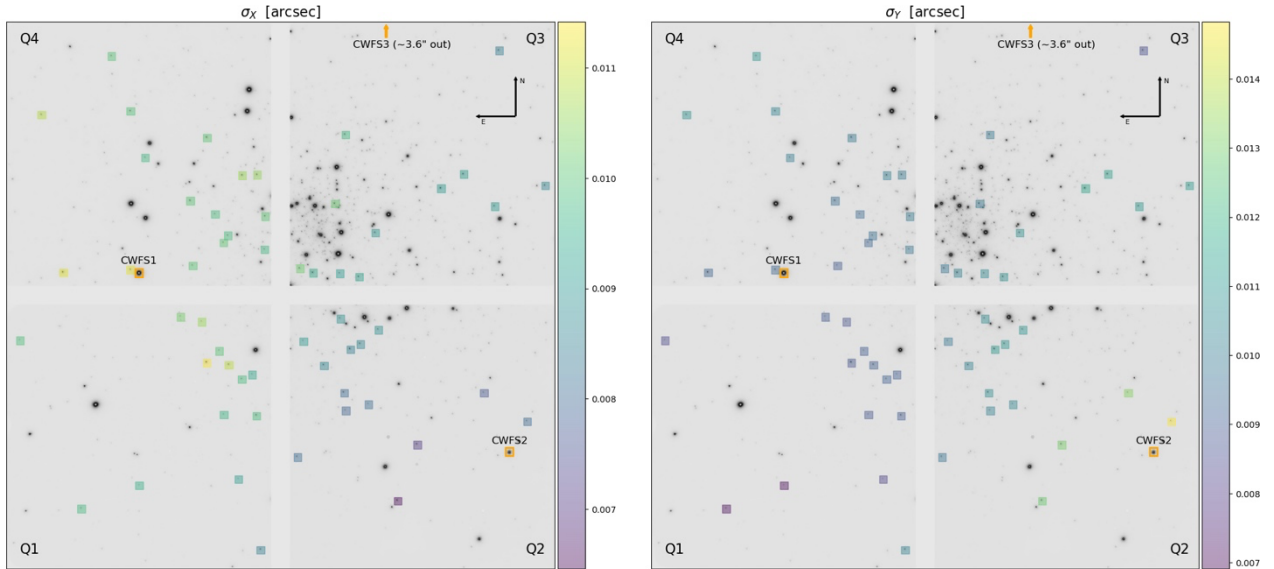


Figure 1. Standard deviations of the measured X and Y centroids from 22 frames taken with the same pointing (NGC 1851) and spanning ~1 hour (one sky offset in between).

Other tests performed that night checked for the stability under nodding/dithering offsets. By nodding by 5-10 arcsec offsets (mimicking ABBA sequences) and regardless of the direction, the measured centroid positions turned out to be recovered mostly well-within half of the pixel scale expected for GeMS+F2. Notice that the smallest slit width expected for this setup is of 2 pixels (~0.17 arcsec), making the observed performance acceptable.

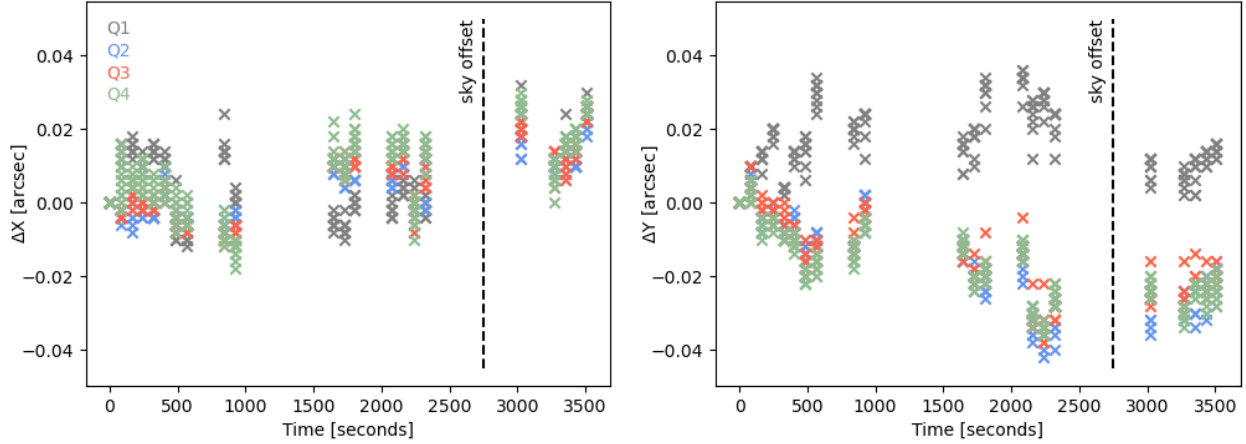


Figure 2. Time evolution of X and Y centroids for the 22 frames observed with GSAOI (relative to the first frame positions). The deviations in centroid positions measured among quadrants in the Y direction are likely attributed to PSF degradation, with the seeing and focus offset worsening as the sequence progressed.

3.2 Spectroscopic observations, data reduction and analysis

The first set of spectroscopic data was taken during the night of April 6th, 2023. For the tests we used the open F/16 Lyot wheel position, the RK3 grism centered on the H-band ($1.65 \mu\text{m}$) and a 4-pix slit width (~ 0.35 and 0.72 arcsec for GeMS+F2 and F2-only setups, respectively). This grism configuration covers approximately from $\sim 15000 \text{ \AA}$ to $\sim 17600 \text{ \AA}$, and a first assessment of the sampling scale gave us $0.087 \text{ arcsec pix}^{-1}$ for GeMS+F2. Only a non-optimal non-common path aberration (NCPA) calibration was applied for the AO; in spite of that, preliminary results can attest the improvement capability of this correction: cuts along the spatial axis around the central wavelength of individual spectra gave us profile widths of ~ 0.56 arcsec and ~ 0.17 arcsec for the seeing-limited (F2-only) and the GeMS+F2 setups, respectively (figure 3, left). A more refined NCPA calibration should further improve the AO-corrected profile. A GeMS+F2 ABBA sequence was also observed with a 2-pix slit width configuration; one of the spectra is shown in figure 3 (right), only calibrated in wavelength through OH sky lines.

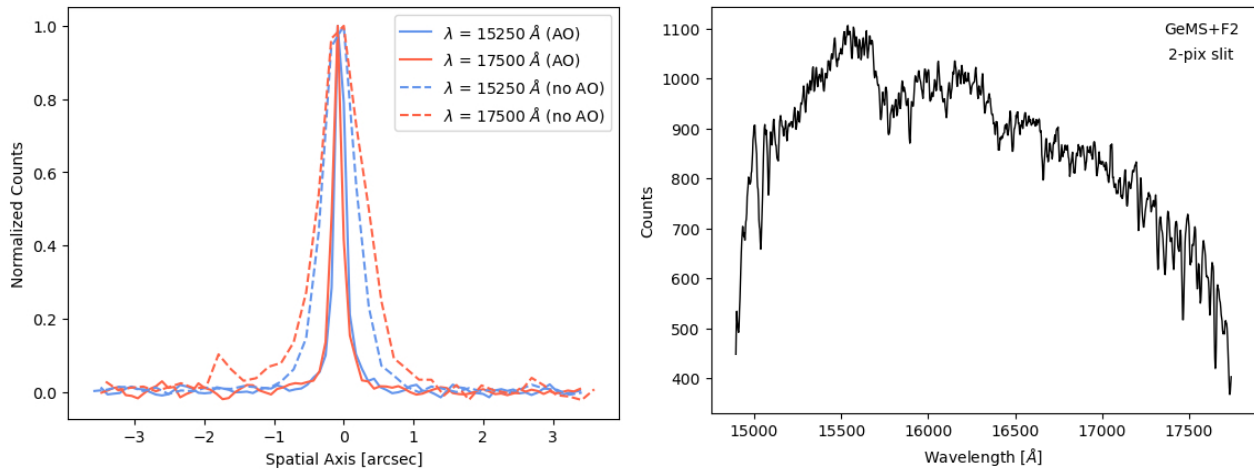


Figure 3. Left: spatial cuts in different positions of individual spectra observed with and without GeMS, at two different wavelengths. Right: example of a spectrum (only calibrated in wavelength) observed with GeMS+F2 using a slit width of 2 pixels.

A second night of engineering with spectroscopy occurred in June 2023. Such data, not presented here, makes an initial attempt to tackle aspects such as thermal background characterization, scattering measurements and spectral resolution in long-slit mode. Even though only counting on H-band observations, preliminary results are promising, pointing towards an improvement with respect to background and scattering contamination with the use of the GeMS+F2 setup. Tests with the 2-pix slit width showed that the spectral resolution ($R = \lambda/\Delta\lambda$) at $\sim 1.62 \mu\text{m}$ with GeMS+F2 resulted in $R \sim 3430$, in accordance to expectations.

3.3 Field distortion characterization

Multi-object spectroscopy relies on a mask design with slits located at the positions of targets spread across the field. The design process can be either based on pre-imaging or on existent catalog images. In the latter case it is necessary to know the field distortions introduced by the instrument. F2 pinhole and Canopus NGS calibration mask images have been taken and used to build the field distortion maps for the GeMS+F2 setup. Both Canopus and F2 contribute to the distortions, and they have been modeled using a Legendre polynomial expansion up to the 3rd order. It turns out that the overall distortion budget is dominated by the second order, affecting mostly one direction of the detector. Figure 4 shows the measured raw map of distortions. However, it is likely that - at least initially - pre-imaging will be the favored basis to design masks.

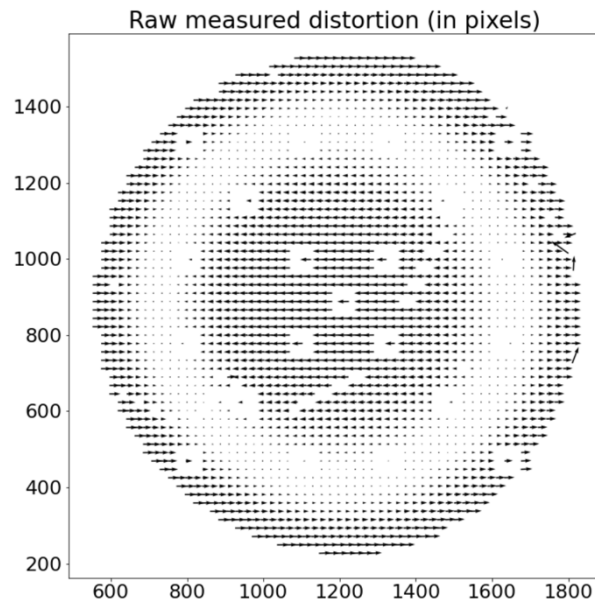


Figure 4. Raw map of distortions for GeMS+F2.

3.4 Non-common path aberrations

The algorithm used for non-common path aberrations (NCPA) calibrations under GSAOI operations is OPRA² ("Optical Transfer Function Phase Retrieval Algorithm", written by Rigaut F., Neichel B. and Gratadour D.), and the current plan is to continue using it with F2. However, and as mentioned before, the GeMS+F2 setup produces a pixel scale of $0.087 \text{ arcsec pix}^{-1}$, highly undersampling the AO-corrected PSFs. We opted to continue working with the same defocus amplitude for phase diversity ($\pm 400 \text{ nm rms}$) and to reconstruct the aberrated images using super-resolution (SR) in order to achieve a pixel scale close to that given by GSAOI. In this scenario, changes to OPRA are minimal and just require as input the reconstructed images with a factor 4 increased resolution. For adapting the configuration file of the phase diversity code, GeMS+GSAOI and GeMS+F2 images of the Canopus pinhole mask were compared regarding geometrical aspects, and reference stars and positions identified.

² <https://github.com/frigaut/yorick-opra>

For the reconstruction itself, it is possible to feed multi-frame SR algorithms with Canopus NGS pinhole mask images displaced by fractions of a pixel, being these displacements driven by the tip-tilt mirror. The uncertainty in such small induced offsets is not an issue, with registration algorithms performing well in their estimation. A variety of multi-frame SR algorithms is currently available, but we have focused so far on the Fast and Robust SR method proposed by [6]. This study is ongoing but preliminary results are encouraging. Figure 5 shows a SR estimation of 9 defocused Canopus pinhole mask "stars" observed with GeMS+F2.

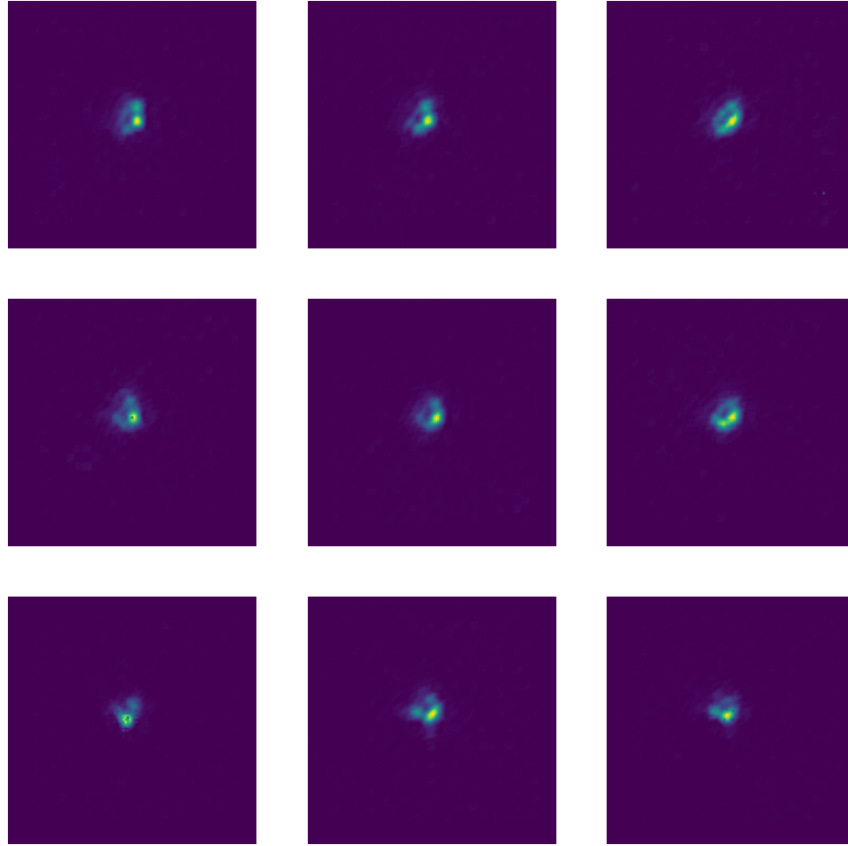


Figure 5. Example of SR reconstruction of the defocused images of 9 stars from the Canopus pinhole mask.

4. NEXT STEPS

The feasibility study shall be concluded by the end of September 2023. A non-exhaustive list for the follow-up of this study comprises:

- Further testing of the SR and NCPA algorithms.
- Ensure centroid and encircled-energy stability across the FoV (critical for MOS). This goes along with GeMS goals such as addressing WFS optical alignment issues and making improvements on the MCAO anisoplanatic mode. Flexures and differential refraction effects also need to be further investigated.
- Improve acquisition (slit alignment) and spectral calibration procedures.
- Introduce changes to the observatory tools so they can accommodate this new mode of operation.
- Fully characterize the GeMS+F2 throughput and the background contamination for all Lyot mask configurations and in different filters.
- Have the MOS mask design algorithm adapted for GeMS+F2.

- Study reconstruction strategies for better tuning the GeMS performance for the long-slit and MOS cases.

REFERENCES

- [1] Rigaut F., et al., "Gemini multiconjugate adaptive optics system review – I. Design, trade-offs and integration", *Monthly Notices of the Royal Astronomical Society*, Volume 437, Issue 3, 21 January 2014, Pages 2361–2375.
- [2] Neichel B., et al., "Gemini multiconjugate adaptive optics system review – II. Commissioning, operation and overall performance", *Monthly Notices of the Royal Astronomical Society*, Volume 440, Issue 2, 11 May 2014, Pages 1002–1019.
- [3] McGregor P. et al., Proc. SPIE, 5492, Ground-based Instrumentation for Astronomy, 1033 (2004).
- [4] Carrasco E.R. et al., Proc. SPIE 8447, Adaptive Optics System III, 84470N (2012).
- [5] Rousselot et al., 2000, A & A, 354, 1134.
- [6] Farsiu, S., Dirk Robinson, M., 2004, IEE Transactions on Image Processing, vol. 13, no. 10.